

Accepted Manuscript

Microstructure, mechanical properties and wear performance of AZ31 matrix composites reinforced by graphene nanoplatelets(GNPs)

Liqun Wu, Ruizhi Wu, Legan Hou, Jinghuai Zhang, Milin Zhang



PII: S0925-8388(18)31321-5

DOI: [10.1016/j.jallcom.2018.04.035](https://doi.org/10.1016/j.jallcom.2018.04.035)

Reference: JALCOM 45673

To appear in: *Journal of Alloys and Compounds*

Received Date: 23 November 2017

Revised Date: 25 March 2018

Accepted Date: 3 April 2018

Please cite this article as: L. Wu, R. Wu, L. Hou, J. Zhang, M. Zhang, Microstructure, mechanical properties and wear performance of AZ31 matrix composites reinforced by graphene nanoplatelets(GNPs), *Journal of Alloys and Compounds* (2018), doi: 10.1016/j.jallcom.2018.04.035.

This is a PDF file of an unedited manuscript that has been accepted for publication. As a service to our customers we are providing this early version of the manuscript. The manuscript will undergo copyediting, typesetting, and review of the resulting proof before it is published in its final form. Please note that during the production process errors may be discovered which could affect the content, and all legal disclaimers that apply to the journal pertain.

Microstructure, mechanical properties and wear performance of AZ31 matrix composites reinforced by graphene nanoplatelets(GNPs)

Liqun Wu^{1,3}, Ruizhi Wu^{1,2,*}, Legan Hou¹, Jinghuai Zhang¹, Milin Zhang^{1,2}

1. Key Laboratory of Superlight Materials & Surface Technology, Ministry of Education, Harbin Engineering University, Harbin 150001, China

2. College of Science, Heihe University, Heihe 164300, P.R. China

3. College of Materials and Engineering, Heilongjiang University of Science and Technology, Harbin 150022, China

Abstract: AZ31 magnesium matrix composites reinforced by nickel coated graphene nanoplatelets (denoted as Mg-3wt.% Al-1wt.% Zn-0.5wt.% GNPs) were fabricated with vacuum hot-press sintering process. The sintered compacts were then hot extruded at 390°C. The microstructure, mechanical properties and wear performance were investigated. The results show that, the nickel coated GNPs uniformly distribute in the matrix. The compressive strength, microhardness, the coefficient of friction and wear rate of the composites are noticeably improved, compared to the matrix alloy of AZ31. GNP content is the main factor affecting the wear behavior of composites, and the addition of GNPs resulted in a significant increase of the abrasion resistance and a decrease of the friction coefficient.

Key words: GNPs, AZ31, microhardness, compressive strength, wear performance

1. Introduction

Magnesium and its alloys are widely used in aerospace, automobile manufacturing, as well as electronic and consumer product related industries, because of its superior physical properties^[1-2]. However, magnesium and its alloys possess poor mechanical properties and wear resistance^[3], which is the bottleneck of their further development and application. To improve the mechanical properties and wear resistance of magnesium alloys, some reinforcements are added into magnesium alloys. The reinforcements can be ceramic or intermetallic compound, such as Al₂O₃, TiB₂, Fe₃Al, Ni₃Al, Al₃Ni₂, Ti₃Al, etc^[4-7]. However, due to the brittleness of these reinforcements, the improvement of mechanical properties and wear resistances is somewhat limited^[8-10]. Recently, graphene has been becoming one of research hot spots, because of its excellent properties in thermal and electric conductivity, lubricating, and mechanical performance. The tensile strength and elastic modulus of graphene are 125 GPa and 1100 GPa, respectively^[11-13]. Accordingly, graphene is a good candidate for the reinforcement in metallic matrix composite to obtain good conductivity, high mechanical properties and high wear resistance due to the self-lubricating^[14-17].

Currently, the studies of metal matrix composite reinforced with GNPs focus on Al and Cu. The researchers^[18-20] prepared the GNPs/Al composites by powder metallurgy technique and ball-milling techniques, the tensile strength and bending strength of composites had a significantly improvement. Kim et al.^[21] demonstrated a new material design in the form of a nanolayered composite consisting of alternating layers of copper and monolayer graphene that has ultra-high strengths of 1.5 and 4.0 GPa. Chen, et al.^[22] have fabricated the GNPs/Mg by a novel nanoprocessing method (liquid state ultrasonic processing and solid state stirring), and founded the microhardness of Mg base nanocomposites reinforced with 1.2 vol.% GNPs is 78% higher than the hardness of pure Mg. However, compared with the GNPs/Al composites, research on GNPs/Mg composites is relatively few.

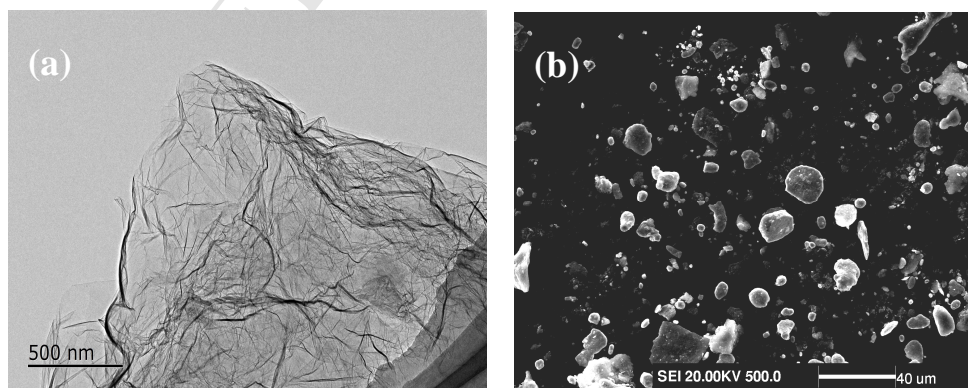
In the preparation of magnesium matrix composite reinforced by GNPs, how to improve the wettability between graphene and magnesium and obtain a homogenous dispersion of graphene in magnesium is the two key points.

In this paper, Mg-3wt.%Al-1wt.%Zn-0.5wt.% GNPs composites were prepared with vacuum hot pressing sintering and hot extrusion. The microstructure, mechanical properties and wear performance of the composites were investigated.

2. Experimental

2.1 Materials

The Mg, Al and Zn powders with particle sizes from 1 μ m to 40 μ m and a purity of 99.95% are used as the raw materials for AZ31 matrix. The used GNPs have average layers less than 10, purity \geq 99wt.%, ash content \leq 0.1wt.%, specific surface area 90~150 m²/g, average thickness $<$ 7nm, flake diameter is 30 μ m~40 μ m and electrical conductivity $>$ 104 S/m. The microstructures of raw GNPs are shown in Fig. 1.



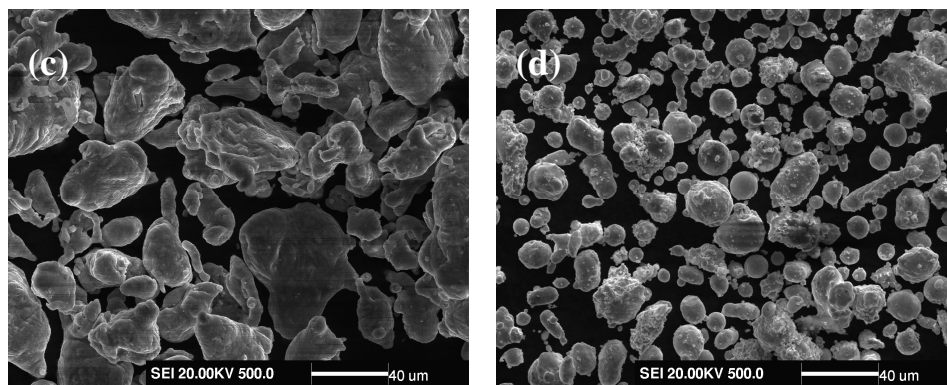


Fig.1. Micrographs images of composite powders:

(a) TEM of GNPs, (b) SEM of Mg powder, (c) SEM of Al powder, (d) SEM of Zn powder

2.2 Processing

2.2.1 Preparation of mixed powder

GNPs were cleaned with ultrasonic treatment, then they undergo an acidification treatment in the mixture of H_2SO_4 and HNO_3 (1:3 by volume), causing the formation of useful functional groups on GNPs surface such as carbonyl group ($>\text{C}=\text{O}$), hydroxyl ($-\text{OH}$) and carboxyl ($-\text{COOH}$), and removal of impurities from GNPs surface. Sensitization and activation were then carried out in a solution of SnCl_2 and PdCl_2 . The deposition of colloidal Sn^{2+} particles onto the surface of the GNPs formed the sensitization step. Sensitized GNPs were activated following the reduction reaction between Pd^{2+} and Sn^{2+} that produced palladium nanoparticles. The palladium nanoparticles serve as centers for catalytic activity during nickel plating. The plating solution contained $\text{C}_6\text{H}_5\text{O}_7\text{Na}_3 \cdot 2\text{H}_2\text{O}$, NH_4Cl , $\text{NiSO}_4 \cdot 6\text{H}_2\text{O}$ and $\text{NaH}_2\text{PO}_2 \cdot \text{H}_2\text{O}$, and the pH was adjusted to within the range 8-9 using $\text{NH}_3 \cdot \text{H}_2\text{O}$. Nickel from solution was reduced and deposited as particles at the active sites, forming a continuous nickel layer on the surface of the GNPs^[23] slowly.

The electroless nickel plated GNPs were then mixed with powders of Al and Zn in a certain proportion, using the low energy ball mill. The mixture powder without Mg is named precursor, which combined with powder of Mg under ultrasonic dispersion and mechanical stirring orderly, to obtain the uniform composite powder. Finally, the composites powder was obtained as the raw material of cold pressing and vacuum hot-pressing sintering by vacuum filtration and vacuum drying.

2.2.2 Vacuum hot-pressing sintering

The homogeneous mixture powder was put in a stainless steel die and pressed under a hydraulic pressure of 300MPa holding for 3mins, to obtain a preform with dimensions of $\text{Ø}30 \times 10\text{mm}$. The preform was sintered in a vacuum hot pressure sintering furnace (ZT-40-20Y). The hot press sintering procedure is shown in Fig. 2.

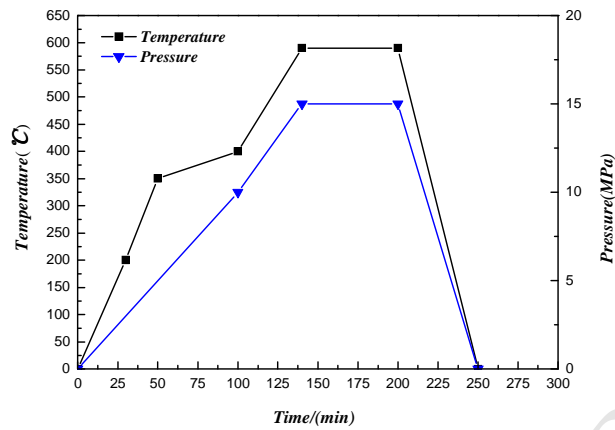


Fig. 2. Schematic illustration of the sintering procedure

2.2.3 Hot extrusion

The sintered specimen was extruded at a temperature of 400°C in a stainless steel die, to obtain the cylindrical rods under a hydraulic press after preheating 400°C for 1h to ensure that the die temperature is consistent with the billet temperature. The extrusion ratio and ram speed were set at 14:1 and 10mm/s, respectively. The specimen of AZ31 has been prepared with use of the above described processes.

The contact area of billet and extrusion die is large, and the speed of deformation is high, so in order to obtain the uniform extrusion speed and reduce the sliding friction between the billet and die, the inwall of die were evenly coated with graphene.

2.3 Microstructure characterization

The Raman spectra for GNPs and GNPs+Ni were measured with Raman spectrometer (HR-800) in the range of 0-3000 cm^{-1} with a wavelength of 514nm.

Transmission Electron Microscope (TEM) and scanning electron microscopy (SEM) were employed for microstructure observation. The specimens for raw AZ31 and Mg-3wt.%Al-1wt.%Zn-0.5wt.%GNPs were polished to analyze the microstructures of the GNPs, powders and composites.

X-ray diffraction (XRD) was used to investigate phase analysis of specimens. In the measurement, Cu Ka radiation was used at 40 KV and 30 mA with a scan rate of 0.02 deg/s in a range of 10 - 90°.

2.4 Mechanical properties

The measurement of microhardness was carried out by the microhardness tester. Before measurement, the specimen was successively ground with 100-4000 grit papers and polished with Al_2O_3 , then corroded by 4%

mixed solution of HNO_3 and ethanol for 10 seconds. Five trails were taken across the polished surface of each specimen and the average value is employed.

The compressive properties were tested under an initial strain rate of 5 mm/min with the dimensions $\varnothing 8 \times 15$ mm.

2.5 Wear test

The tribological tests were performed at room temperature (25°C) using the standard pin-on-disc wear testing equipment (THV-5D), under a normal load of 15N at a sliding speed of 0.05 m s^{-1} for 3000 s, the dimension of specimen is $8 \text{ mm} \times 2 \text{ mm} \times 10 \text{ mm}$. The morphologies of wear scars were observed by SEM.

3. Results and discussion

3.1 Microstructure of GNPs and powders

The microstructures of GNPs with and without nickel plating are shown in Fig. 3. Almost all the GNPs are separated from each other, as shown in Fig. 3 (a). The surface of GNPs with nickel plating is rougher than the GNPs before nickel plating, as shown in Fig. 3 (b). EDS result shows that GNPs were coated by nickel particles.

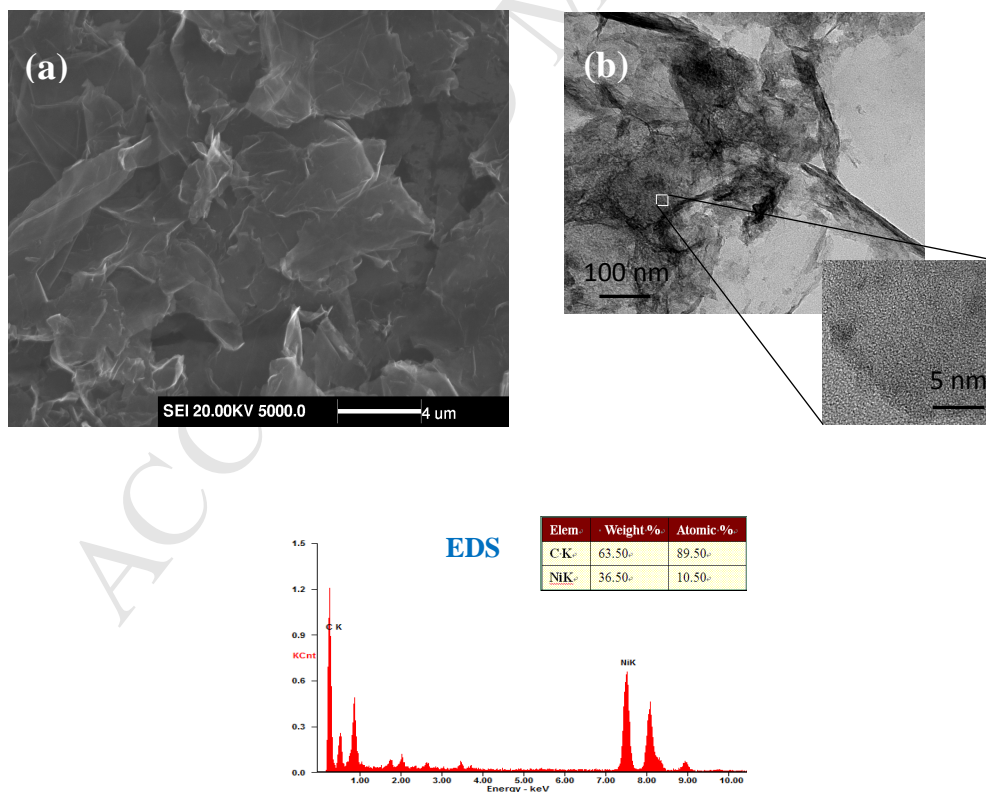


Fig. 3. The images and EDS results for GNPs +Ni: (a) SEM of GNPs, (b) TEM of GNPs + Ni, (c) EDS of (b)

Fig. 4 shows the Micrographs and EDS of precursor powders, it is clear that, most of GNPs attach on the

surface of powders of Al and Zn, and only a few single GNPs scatter around powders. This characteristic is favorable for uniform distribution of GNPs in magnesium powders.

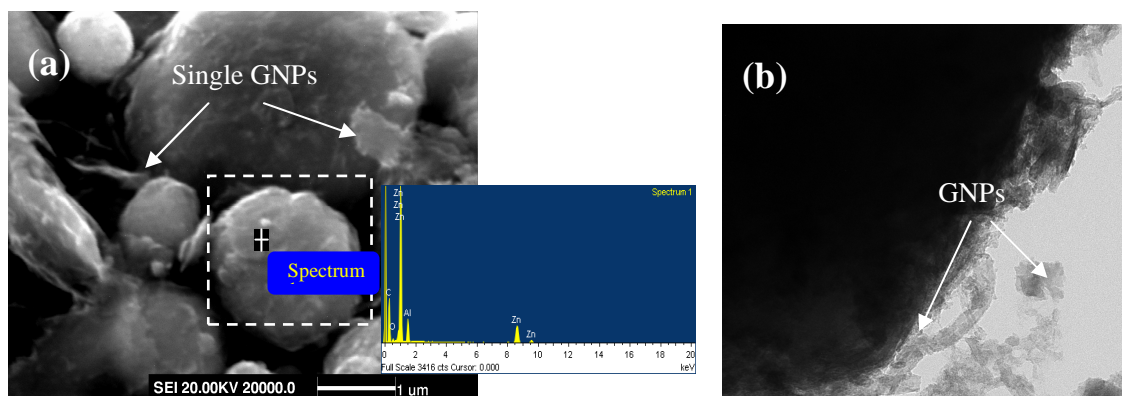


Fig. 4. Micrographs of composite precursor powder: (a) SEM image, (b) TEM image

Raman spectra of GNPs and GNPs+Ni are shown in Fig. 5. There exist D peak (disorder related^[24]) at 1349 cm^{-1} , strong G peak (graphite related^[25]) at 1580 cm^{-1} , a broad second order 2D peak at 2689 and 2685 cm^{-1} . Compared to the GNPs, the intensities of D peak and G peak of GNPs+Ni decrease, indicating that the surface structure of GNPs is damaged partially due to Ni plating^[26]. Meanwhile, the intensity ratio of I_D/I_G decreases from 0.77 for GNPs to 0.64 for GNPs+Ni, indicating the addition of oxygenated groups for GNPs, which is conducive to the electroless nickel plating^[27]. The locations of G peak and 2D peak move left wards after nickel plating indicating more uniform dispersion.

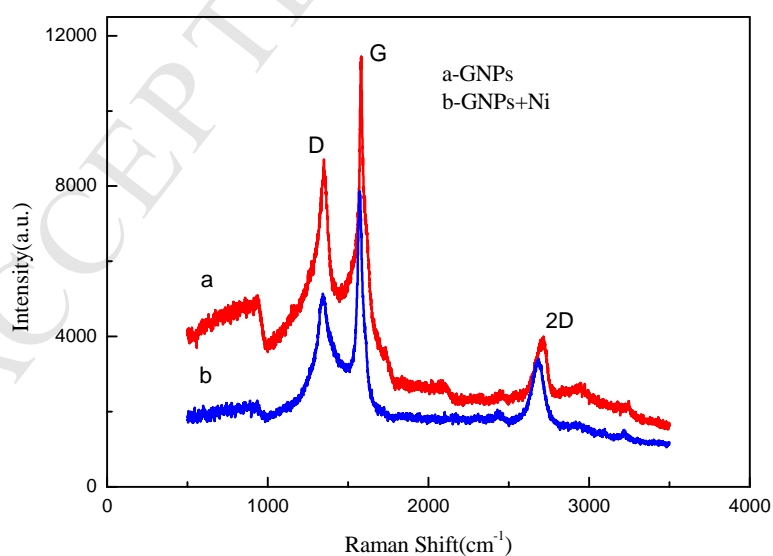


Fig. 5. Raman spectra of GNPs, (a) raw GNPs, (b) GNPs+Ni

3.2 Microstructure of AZ31 and (GNPs+Ni)/AZ31

The SEM images of AZ31 and GNP/AZ31 are shown in Fig. 6. It can be seen that the grain size of the α -Mg matrix becomes smaller with adding 0.5% GNPs. This indicates that reinforcement can play a role in refining matrix grains because GNPs that distribute at the grain boundary can hinder grain growth. Micrographs of AZ31 and GNP/AZ31 revealed some micropores on the specimen surface, which is because the grain refinement is not uniform in matrix. This may be attributed to poor dispersion of two dimensional GNPs reinforcement in the matrix. It is clear that the surface of GNP+Ni/AZ31 is smooth and the grain boundaries is clear, as shown in the Fig. 6 (c). It is indicated that, there is a good bonding existed between nickel coating GNPs and the matrix.

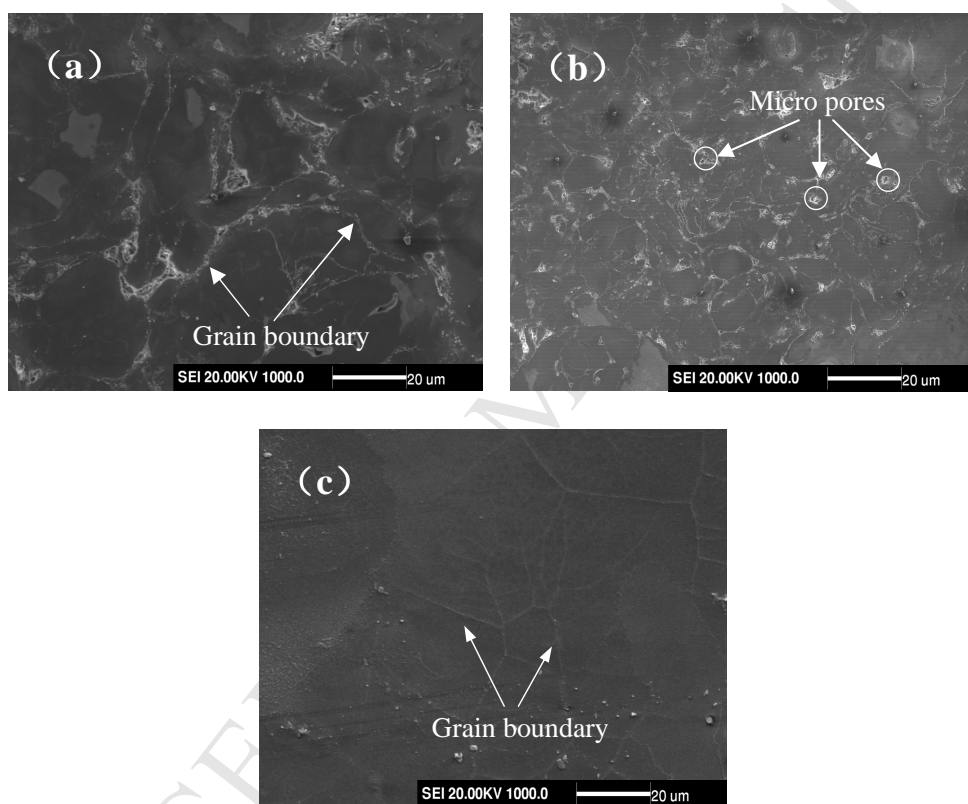


Fig. 6. Micrographs of investigated AZ31 and its composites
(a) AZ31, (b) GNP/AZ31, (c) GNP+Ni/AZ31

3.3 Mechanical properties

Fig.7 shows the microhardness values of AZ31, 0.5wt.%GNP/AZ31 and 0.5wt.% (GNP+Ni)/AZ31. The microhardness value of 0.5wt.%GNP/AZ31 increases by 24.51% compared to AZ31, and the increases of 0.5wt.% (GNP+Ni)/AZ31 compared to AZ31 and 0.5wt.%GNP/AZ31 are 34.71% and 8.2%, respectively.

GNPs can restrict the localized deformation during indentation causing the increase of hardness. In addition, nickel plating improves the interface binding between GNPs and magnesium matrix. Accordingly, the hardness value of (GNP+Ni)/AZ31 is higher than that of GNP/AZ31.

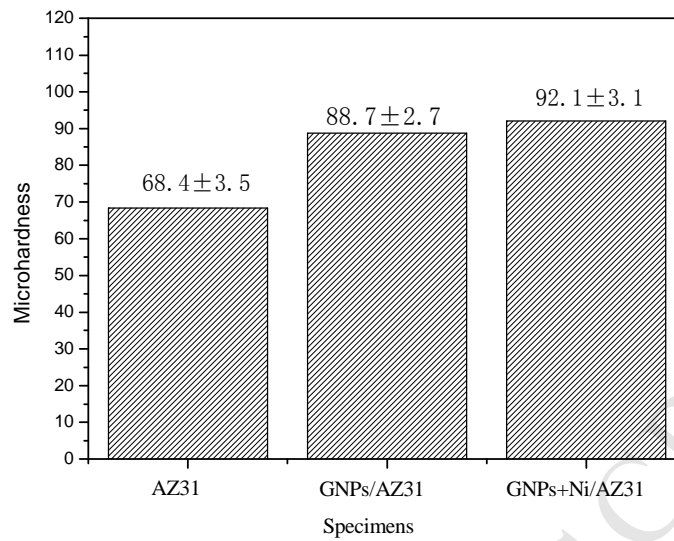


Fig.7. Microhardness value of AZ31, 0.5wt.%GNPs/AZ31 and 0.5wt.%(GNPs+Ni)/AZ31

Compressive properties of AZ31, 0.5wt.%GNPs/AZ31 and 0.5wt.%(GNPs+Ni)/AZ31 are shown in Table 1. AZ31 reinforced by GNPs can improve both strength and plasticity. The process of nickel plating can further improve the compressive properties.

Tab.1 Room temperature compressive properties of AZ31 and its composites

Materials	0.2% CYS (MPa)	UCS (MPa)	d (%)
AZ31	163	341	8.62 ± 0.24
0.5wt.%GNPs/AZ31	196	381	9.10 ± 0.22
0.5wt.%(GNPs+Ni)/AZ31	221	402	10.55 ± 0.15

CYS: compressive yield stress; UCS: ultimate compressive stress; d: strain to failure.

3.4 Wear properties

Fig. 8 shows the coefficient of friction (COF) and wear rate (WR) as a function of the sliding time. As shown in Fig. 8 (a), the COF value of AZ31 is gradually stabilized at ~0.47 after a short running-in period (<320s), due to the removal of thin MgO film on the surface.^[28] Compared with the high COF value of AZ31, the value is decreased to ~0.26 in the GNPs/AZ31 specimen in the initial stage (<200s), and then it begins to increase and eventually reaches the value of ~0.36, which decreases by 23.4% compared to AZ31. Because the binding between GNPs and matrix is relatively poor without the nickel plating, GNPs cannot offer a continuous good lubrication during wearing. In contrast, the COF of the (GNPs+Ni)/AZ31 specimen starts at ~0.2 and increases gradually. It

reaches the peak of ~ 0.39 at 600s, and then continuously decrease with a final COF of ~ 0.26 . This is because the nickel layer surface is rough, leads to the higher value of COF of the (GNPs+Ni)/AZ31 in the initial stage. As the nickel layer spalling from the surface constantly, the graphene appears at the surface, and the value of COF begins to reduce, and tends to be stable after the 1800 s.

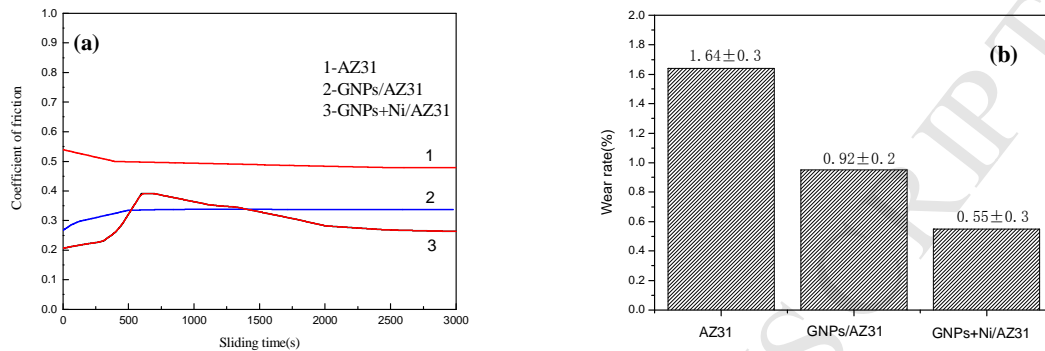


Fig.8 (a) coefficient of friction and (b) wear rate of AZ31, GNPs/AZ31 and (GNPs+Ni)/AZ31

Fig.8 (b) shows the influence of GNPs on the wear resistance value. The wear resistance value of 0.5wt.% GNPs/AZ31 decreases by 43.9% compared with AZ31, due to the lubrication of GNPs. The wear rate of 0.5wt.% (GNPs+Ni)/AZ31 notably decreases to 0.55, which reduce by 66.46% and 40.22%, respectively, compared with AZ31 and 0.5wt.% GNPs/AZ31. It can be explained that, nickel coating graphene can combine with magnesium matrix better and stronger. Accordingly, the lubrication effect of the grapheme becomes better, resulting in the decrease of the amount of wear and tear obviously.

Fig. 9 shows the microstructure of the worn out surface. The worn out surfaces of the specimens are covered with rows of furrows parallel to the sliding direction, as shown in Fig. 9 (a) to (c). There are some hard asperities and particles on the steel counterface, which plough and cut into the surface causing wear by the removal of small fragments or ribbon-like strips of composites. The appearance of smooth stripes illustrates the serious plastic deformation of the specimens produced in the sliding. These typical features represent the typical abrasive wear behavior.^[29] Compared with AZ31, the number of debris in the GNPs/AZ31 and (GNPs+Ni)/AZ31 samples are markedly decreased, and the phenomenon of delamination is also reduced.

It is clear from Fig.9 (c) and (d) that, GNPs disperse uniformly on the wear surface with little debris and furrows, which infers that the presence of GNPs is beneficial to reduce wear rate, due to the low shear force and friction coefficient between graphene layers.

The typical mechanisms associated with the abrasive wear for (GNPs+Ni)/AZ31 can be summarized as follows: (i) The GNPs are crushed forming a carbon film, which covers the surface and acts as a solid lubricant,

reducing the COF of composites. (ii) The excellent thermal conductivity of GNPs improves the thermal conductivity of the matrix,^[30] which releases the heat generation and maintains the hardness and strength of the composite in the wear test. (iii) The fraction of the GNPs on the specimen surface increases with GNPs addition, the contact area between the matrix and the disk decreases, thus contributing to the reduction of the COF.

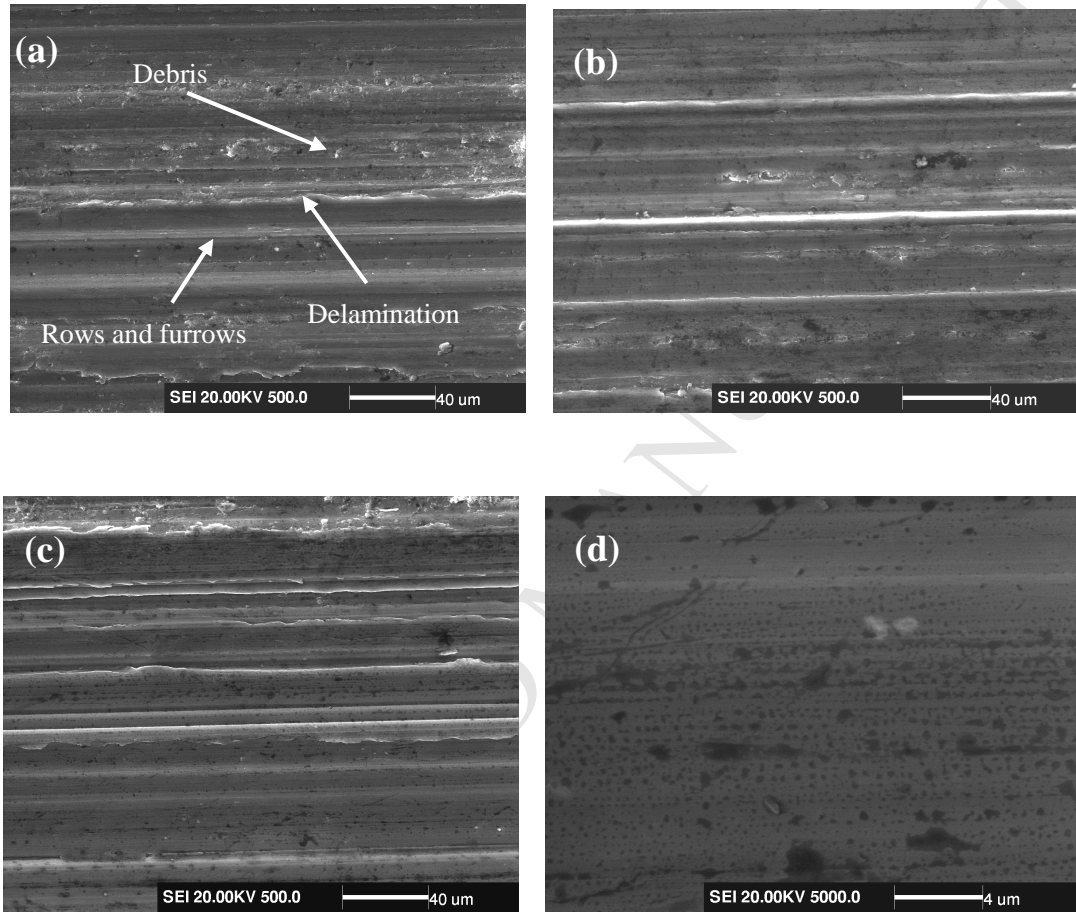


Fig.9 SEM images of wear tracks for (a) raw AZ31, (b) GNPs/AZ31, (c) GNPs+Ni/AZ31, (d) high resolution of (c)

To sum up, the hardness and COF are two key factors influencing wear properties of materials, the highest hardness and the least wear mass lead to the best wear resistance, as described by the following Archard equation^[31]:

$$WR_v = ld \frac{f}{h}$$

Where WR_v is worn volume; l is the value of load; d is the sliding distance; f is the COF; h is the value of hardness.

The worn volume of AZ31 and its composites are provided in Tab.2. It is clear from the Tab.2 that the experimental values of AZ31 and GNPs/AZ31 composites worn volume are slightly higher than their theoretical

values and the experimental value of (GNPs + Ni)/AZ31 is lower than its theoretical value. The experimental results show that the GNPs after dealing with the nickel plating can effectively reduce the worn volume of composites, and the experimental value is lower than the theoretical value. It is maybe because that, the Archard equation cannot analyze the role of nickel layer in improving the interface bonding between GNPs and matrix in the friction test. The calculated results show that the relationship of the wear rate, microhardness and coefficient of friction of AZ31 and its composites are consistent with the Archard equation.

Tab.2 The worn volume of AZ31 and its composites

Materials	Experiment value	Theoretic value	Error (%)
AZ31	1.82	1.55	15.052
GNPs/AZ31	0.99	0.91	7.759
GNPs+Ni/AZ31	0.61	0.64	-4.128

4. Conclusion

1. The pre-processed GNPs are homogenous distributed, and uniformly coated by nickel with the electroless plating. After nickel plating, the structure of GNPs keeps integrity with little damage.
2. The (GNPs+Ni)/AZ31 composite prepared by vacuum hot-pressing sintering followed with hot extrusion exhibits a significantly improvement on the microhardness, compressive properties and wear properties.
3. Compared with AZ31 and GNPs/AZ31, the (GNPs+Ni)/AZ31 composite has a lower coefficient of friction and wear rate. The wear type of (GNPs+Ni)/AZ31 composite is an abrasive wear behavior.

This paper was supported by National Natural Science Foundation(51671063 , 51771060),Research Fund for the Doctoral Program of Higher Education (20132304110006),Heilongjiang Province Natural Science Foundation (ZD2017010), the Fundamental Research Funds for the Central Universities (HEUCFM171007),Harbin City Application Technology Research and Development Project(2015AE4AE005, 2015RQXXJ001, 2016AB2AG013).

Reference:

- [1]R. Z. Wu, Y. Yan, G. Wang, L. E. Murr, W. Han, Z. Zhang and M. L. Zhang, *Int. Mater. Rev.*, 60 (2015) 65-100.
- [2]X. J. Wang, D. K. Xu, R. Z. Wu, X. B. Chen, Q. M. Peng and L. Jin et al., *Mater. Sci. Technol.*, Doi: 10.1016/j.jmst. (2017).07.019.
- [3]R. Gadow, D. Scherer, *Surf. Coat. Technol.*, 151 (2002) 471-477.
- [4]P. Z. Shen, H. Y. Gao and M. Song, et al., *J. Mater. Eng. Perform.*, 22 (2013) 3959-3966.
- [5]J. W. Qian, J. L. Li and J. T. Xiong, et al., *Mater. Sci. Eng., A*, 550 (2012) 279-285.
- [6]L. G. Hou, R.Z. Wu, X.D. Wang, J.H. Zhang, M.L. Zhang, A.P. Dong and B.D. Sun, *J. Alloy. compd.*, 695 (2017) 2820-2826.
- [7]L. G. Hou, B. C. Li, R. Z. Wu, L. Cui, P. Ji, R. Y. Long and J. H. Zhang et al., *J. Mater. Sci. Technol.*, 33 (2017) 947-953.
- [8]H. Ferkel and B.L. Mordike, *Mater. Sci. Eng. A* 298 (2001) 193-199.
- [9]R. A. Saravanan and M. K. Surappa, *Mater. Sci. Eng. A*, 276 (2000) 108-116.
- [10]C. G. Lee, X. D. Wei, and J. W. Kysar et al., *Sci.*, 321 (2008) 385-388.
- [11]M. K. Habibenjad, R. Mahmudi, H. M. Ghasemia and W. J. Poole, *Wear*, 168 (2010) 405-412.
- [12]H. Q. Li, Y. T. Xie and K. Li, et al., *Ceram. Int.*, 40 (2014) 12821-12829.
- [13]J. Y. Wang, Z. Q. Li and G. L. Fan, et al., *Scr. Mater.*, 66 (2012) 594-597.
- [14]M. Bastwros, G. Y. Kim, and C. Zhu an et al., *Composites Part B*, 60 (2014) 111-118.
- [15]J. M. Ju, G. F. Wang, and K. H. Sim, *J. Alloy. compd.*, 704 (2017) 585-592.
- [16]H. A. S. Shin, J. Ryu, S. P. Cho, E.K. Lee, S. Cho C. Lee Y. C. Joo, and B. H. Honget al., *Phys. Chem. Chem. Phys.* 16 (2014) 3087-3094.
- [17]Y. K. Chen, X. Zhang, E. Z. Liu and C.N. He et al., *J. Alloys Compd.*, 688 (2016) 69-76.
- [18]J. Y. Wang, Z. Q. Li, G. L. Fan, et al., *Scr. Mater.*, 66 (2012) 594-597.
- [19]M. Bastwros, G. Y. Kim, C. Zhu, et al., *Composites Part B*, 60 (2014) 111-118.
- [20] S. J. Yan, S. L. Dai., X. Y. Zhang, et al, *Mater. Sci. Eng. A*, 26 (2014) 440.
- [21]Y. Kim, J. Lee, M. S. Yeom, et al., *Nat Commun*, 4 (2013) 2114.
- [22]L. Y. Chen, H. Konishi and A. Fehrenbacher, et al., *Scripta Materialia*, 67 (2012) 29-32.
- [23]L. Q. Wu, R. Z. Wu, L. G Hou, J. H. Zhang, J. F Sun and M. L. Zhang, *J. Mater. Eng. Perform.*, 26 (2017) 5495-5500.
- [24]A. C. Ferrari, *Solid State Commun.*, 143 (2007) 47-57.
- [25]A. C. Ferrari, J. C. Meyer and V. Scardaciet.al., *Phys. Rev. Lett.*, 97 (2006) 187401.
- [26]C. Thomsen and S. Reich, *Phys. Rev. Lett.*, 85 (2000) 5214.
- [27]L. J. Huang, and Y. X. Wang et al., *Mater.Lett.*, 160 (2015) 104-108.
- [28]L. B. Tong, J. B. Zhang, C. Xu and X. Wang et al., *Carbon* 109 (2016) 340-351.
- [29]M. M. H. Bastwros, A. M. K. Esawi and A. Wifi, *Wear* 307 (2013) 164-173.
- [30]M. srinivasan, C. Loganathan, M. Kamaraj, Q.B. Nguyen, M. Gupta, and R. Narayanasamy, *Trans. Nonferrous Met. Soc. China* 22 (2012) 60-65.
- [31]H. C. Meng, and K. C. Ludema, *Wear* 181 (1995) 443-457.

High lights

1. The GNPs coating by Ni are uniformly distributed, and keep structural integrity.
2. The composite exhibits a improvement on mechanical and wear properties.
3. The composite has a lower COF and wear rate. Its wear type is abrasive wear.